Materials and Design 30 (2009) 2513–2520

Contents lists available at ScienceDirect

Materials and Design

journal homepage: www.elsevier.com/locate/matdes

Extension of *R–K* constitutive relation to phase transformation phenomena

J.A. Rodríguez-Martínez [a,*], A. Rusinek [b], J.R. Klepaczko [c], R.B. Pęcherski [d]

[a] Department of Continuum Mechanics and Structural Analysis, University Carlos III of Madrid, Avda. de la Universidad 30, 28911 Leganés, Madrid, Spain
[b] National Engineering School of Metz (ENIM), Laboratory of Mechanical Reliability (LFM), Ile du Saulcy, 57000 Metz, France
[c] Laboratory of Physics and Mechanics of Materials, UMR CNRS 7554, University Paul Verlaine of Metz, Ile du Saulcy, 57045 Metz, France
[d] Institute of Fundamental Technological Research, Polish Academy of Sciences, ul. Swietokrzyka 21, 00-049 Warsaw, Poland

ARTICLE INFO

Article history:
Received 24 June 2008
Accepted 30 September 2008
Available online 11 October 2008

This paper is dedicated to our friend, Prof. Janusz Roman Klepaczko who passed away in August 15, 2008, for his pioneer contribution in the area of dynamic behaviour of materials.

Keywords:
RK model
Phase transformation
Austenitic steel

ABSTRACT

In this paper an extension of the Rusinek–Klepaczko (RK) constitutive relation is presented. The new formulation proposed, allows defining the phase transformation effect observed on macroscopic scale using a phenomenological approach. The key point is to introduce in the original formulation of RK model a new stress component based on evolution of martensite, which takes into account strain, strain rate and temperature effects. Analytical predictions of the extended constitutive relation are compared with experimental results for 301Ln2B steel. This material is chosen since the phase transformation is well observed during quasi-static loading inducing a strong increase of strain hardening rate during plastic deformation. Satisfactory agreement between analytical and experimental observations has been obtained. The phenomenological extension of RK model allows to reduce substantially the computational time in comparison with models based on physical background, for example [Papatriantafillou I, Agoras M, Aravas N, Haidemenopoulos G. Constitutive modeling and finite element methods for TRIP steels. Comput Methods Appl Mech Eng 2006;195:5094–114]. At the same time, the number of material constants defining the extended RK model is reduced. Seven constants are needed to identify the RK model in its original formulation and five are added for the description of phase transformation process.

1. Introduction

Austenitic steels are of frequent use in several engineering fields, like civil protections, naval structures and others, mostly due to their excellent mechanical properties in terms of high hardening rate, large ductility and toughness [2–8]. Under well defined conditions in terms of stress, strain, strain rate and temperature, these steels reveal phase transformation from austenite to martensite. When phase transformation is induced by plastic deformation, the process is known as TRIP (transformation induced by plasticity) and it has recently achieved a great industrial interest, as it is revealed by large number of papers recently published, for example [9–16]. In order to model the phase transformation phenomena, several constitutive relations can be found in the international literature [17–25]. The most relevant seems to be the approach by Olson and Cohen [9]. This model called OC was later generalized to take into account the stress state effect [10], strain rate [11] and stress state for stacking fault energy [12]. A use of these kind of physical models in FE codes results in long computational time causing limiting industrial applications since these constitutive relations are coupled with a homogenization method as proposed by Aravas [26].

Thus, in the present paper a phenomenological extension of the constitutive relation due to Rusinek and Klepaczko, called RK model [27] is proposed to take into account the phase transformation phenomena. The model reported in the present paper allows obtaining satisfactory agreement with experimental results. The original version of the RK model coupled with the fully implicit algorithm [28] has been previously used by solving numerically several dynamic problems, for example [29–34]. Combination of the extended RK model and the implicit algorithm allows for reduction of computational time in comparison with OC model coupled to the algorithm introduced by Aravas [26]. Those conclusions were reported in [35] after comparison of both constitutive relations, OC model coupled with an homogenization method [26] and RK extended model coupled with a fully implicit algorithm [28], using ABAQUS/explicit. Short computational time and simple formulation makes the extended RK constitutive relation very attractive for numerical applications in industry, where the phase transformation in austenitic steels might be dominant, for example perforation, crash box behaviour or high speed machining. However, the application of this approach does not provide information about microstructure evolution during plastic deformation.

* Corresponding author. Tel.: +34 91 624 8460; fax: +34 91 624 9430.
E-mail address: jarmarti@ing.uc3m.es (J.A. Rodríguez-Martínez).

0261-3069/$ - see front matter © 2008 Elsevier Ltd. All rights reserved.
doi:10.1016/j.matdes.2008.09.043

2. Kinetics of phase transformation and application to modeling

The presence of the phase transformation in austenitic steels during plastic deformation strongly depends on temperature, Fig. 1a. In fact, only under certain loading conditions of strain rate and initial temperature the phase transformation appears.

The phase transformation process can be decomposed in three parts as a function of temperature, Fig. 1a. For temperatures low enough, the phase transformation appears instantaneously without plastic deformation (domain *A*). For intermediate range of temperatures, the phase transformation is induced by plastic deformation (domain *B*). For higher temperature levels, the residual austenite remains stable and no phase transformation is observed.

But also the strain rate exercises a great influence in that process. When austenitic steels are subjected to high strain rate loading, the adiabatic conditions of plastic deformation induce a high temperature increase in the material slowing down or completely eliminating the phase transformation. It is shown in Fig. 1b that for a moderate strain rate level, $\dot{\bar{\varepsilon}}_p = 500\ s^{-1}$ the phase transformation does not appear at room temperature.

The knowledge of the kinetics of the phase transformation is of great interest in several industrial processes as those already mentioned, for example, crash box behaviour. Such structures are commonly used in the automotive industry. They allow absorbing a large amount of energy during direct impacts or collisions.

The main role of phase transformation process in this kind of application is to increase the yield stress level in comparison with steels without phase transformation. Such technological operation is carried out by introduction of a plastic pre-strain into the steel sheet, Fig. 1a. The maximum effect of plastic pre-strain observed in this kind of structure is close to $\bar{\varepsilon}_p = 0.1$. This operation carried out by an extra rolling allows avoiding failure in the sheet due to an excessive plastic deformation. An analysis of this problem has been conducted previously by Durrenberger et al. [36]. Due to quasi-static bending process applied to the steel sheet after pre-strain, in order to form an "omega" shape, Fig. 2b, additional phase transformation effect can appear.

For crash box application it is necessary to define correctly the behaviour of austenitic steel in a range of strain rates varying in the following limits: $\dot{\bar{\varepsilon}} \leq 10^{-3}\ s^{-1}$ to $\dot{\bar{\varepsilon}} \approx 1000\ s^{-1}$. As previously reported, during dynamic loading, due to high temperature increase by adiabatic heating, the austenite remains stable and no phase transformation is observed [12,37]. Thus, the phase transformation must be introduced in modeling before the crash test application.

3. Formulation of the constitutive relation and parametric study of the phase transformation kinetics

The RK constitutive relation [27] is a semi-physical approach taking into account the effects of work-hardening, $\bar{\varepsilon}_p$, strain rate, $\dot{\bar{\varepsilon}}_p$ and absolute temperature, T, on the flow stress $\bar{\sigma}$. It has been previously verified by identification of the thermo-visco-plastic behaviour of several metals as reported in [29,31,34].

3.1. Formulation of the extended RK constitutive relation

In the original formulation of the model, Appendix A, the total stress is decomposed into two terms. The internal stress $\sigma_\mu(\bar{\varepsilon}_p, \dot{\bar{\varepsilon}}_p, T)$ and the effective stress $\sigma^*(\dot{\bar{\varepsilon}}_p, T)$, both components are multiplied by temperature-dependent Young's modulus $E(T)/E_0$ [38]. Such operation takes into account the temperature softening of the crystalline lattice [39]. The original formulation of the RK model is given in Appendix A, [27]. In the present work, a third stress component $\sigma_T(\bar{\varepsilon}_p, \dot{\bar{\varepsilon}}_p, T)$ is added to the RK constitutive relation, which allows approximation of the phase transformation effect using a phenomenological approach. The third component $\sigma_T(\bar{\varepsilon}_p, \dot{\bar{\varepsilon}}_p, T)$ depends on plastic strain $\bar{\varepsilon}_p$, strain rate $\dot{\bar{\varepsilon}}_p$ and temperature, T.

Thus, the general form of the extended RK model is given by Eq. (1)

$$\bar{\sigma}(\bar{\varepsilon}_p, \dot{\bar{\varepsilon}}_p, T) = \frac{E(T)}{E_0}[\sigma_\mu(\bar{\varepsilon}_p, \dot{\bar{\varepsilon}}_p, T) + \sigma^*(\dot{\bar{\varepsilon}}_p, T)] + \sigma_T(\bar{\varepsilon}_p, \dot{\bar{\varepsilon}}_p, T). \quad (1)$$

The third term in Eq. (1) is not normalized by the temperature-dependent Young's modulus.

In order to define the phase transformation effect observed in experiments the following expression for $\sigma_T(\dot{\bar{\varepsilon}}^p, \bar{\varepsilon}^p, T)$ is introduced, Eq. (2)

$$\sigma_T(\dot{\bar{\varepsilon}}^p, \bar{\varepsilon}^p, T) = \sigma_0 \cdot f(\dot{\bar{\varepsilon}}^p, \bar{\varepsilon}^p) \cdot g(T). \quad (2)$$

The first multiplier σ_0 is a fitting parameter which allows defining the maximum of stress increase due to phase transformation, Fig. 3. The multiplier can be estimated by mechanical testing. The value of σ_0 must be identified at the lowest temperature of interest or the lowest temperature of experimental data available. The best solution is performing mechanical testing at $T < M_S$. Thus, it corresponds to the maximum phase transformation observed and therefore to the maximum stress level exhibited by the material. The stress components $\sigma_T(\dot{\bar{\varepsilon}}^p, \bar{\varepsilon}^p, T)$ is split into two independent functions, the effect of plastic strain and strain rate during phase trans-

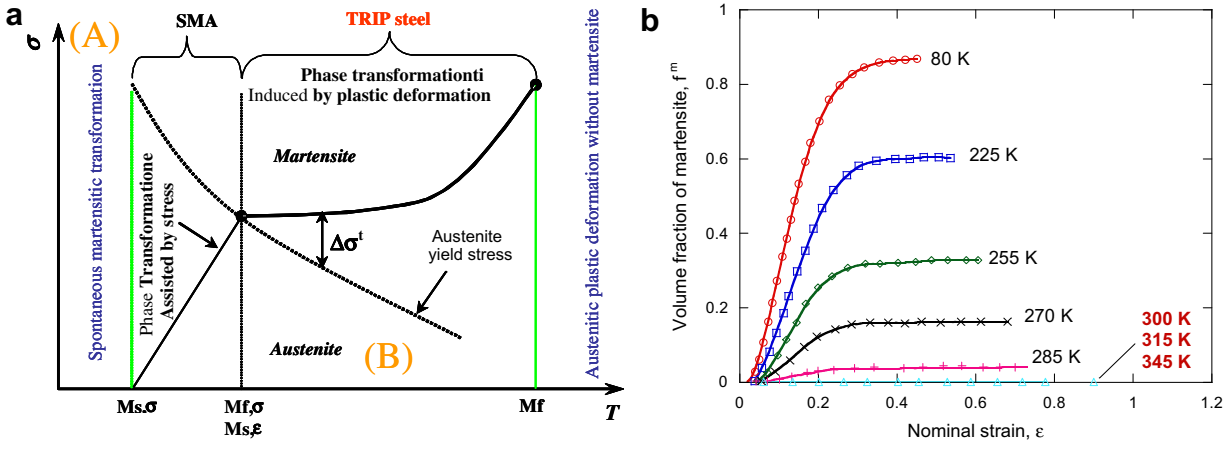

Fig. 1. (a) Schematic description of phase transformation; (b) phase transformation with plastic deformation for different initial temperatures in dynamic loading, 500 s^{-1}, [11].

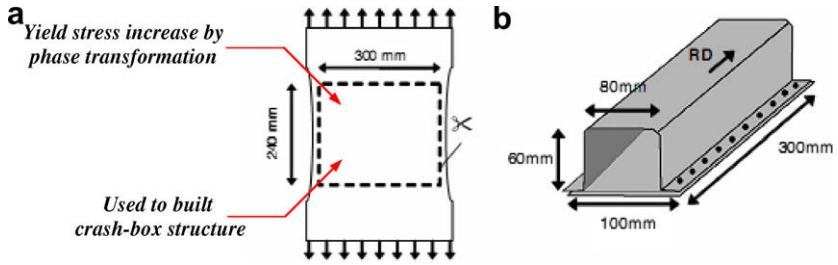

Fig. 2. Prestrain history; (a) specimen dimensions after pre-strain process [36], (b) omega box after bending [36].

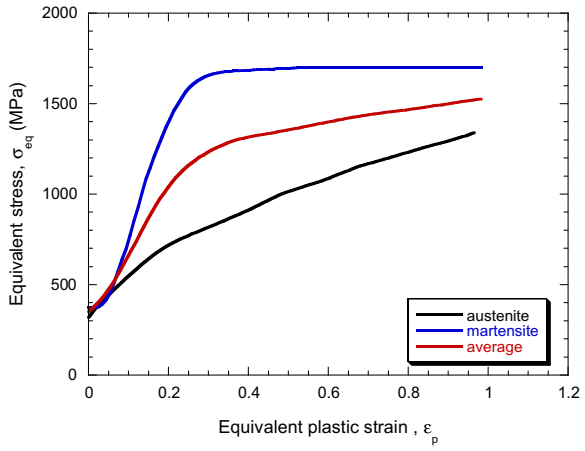

Fig. 3. Mechanical behaviour of different phases [12].

formation, $f(\dot{\bar{\varepsilon}}^{p}, \bar{\varepsilon}^{p})$ and the thermal reduction of the rate of phase transformation $g(T)$.

In case of adiabatic condition the constitutive relation is coupled with heat equation, Eq. (3),

$$T(\bar{\varepsilon}_p, \bar{\sigma}) = T_0 + \frac{\beta}{\rho C_p} \int \bar{\sigma}(\bar{\varepsilon}_p, \dot{\bar{\varepsilon}}_p, T) d\bar{\varepsilon}_p, \tag{3}$$

where β is the Taylor–Quinney coefficient, ρ is the density of the material, C_p is the specific heat and T_0 is the initial temperature. Transition from isothermal to adiabatic conditions in steels is assumed at $\dot{\bar{\varepsilon}}_p = 10\,s^{-1}$ [40]. However, it is possible to include the thermodynamics of phase transformation process as it is reported in details in [37] in order to describe more precisely the temperature increase.

3.2. The effect of plastic strain and strain rate on the phase transformation kinetics

To define the influence of strain and strain rate in the phase transformation, the following function $f(\dot{\bar{\varepsilon}}^{p}, \bar{\varepsilon}^{p})$ is applied, Eq. (4). The expression for $f(\dot{\bar{\varepsilon}}^{p}, \bar{\varepsilon}^{p})$ is similar to the relation with logistic function used in [41,42] to propose phenomenological description of plastic softening of material during the development of multi-scale shear banding. Therefore, the proposed phenomenological description of the plasticity and strain rate effects is given by

$$f(\dot{\bar{\varepsilon}}^{p}, \bar{\varepsilon}^{p}) = [1 - \exp(-h(\dot{\bar{\varepsilon}}^{p})\bar{\varepsilon}^{p})]^{\xi}. \tag{4}$$

One function, $h(\dot{\bar{\varepsilon}}^{p})$, and one material parameter, ξ, are introduced to approximate behaviour of an austenitic steel during the process of phase transformation. Thus, $h(\dot{\bar{\varepsilon}}^{p})$ is defined as being strain-rate dependent in agreement with experimental observations. A decrease of $h(\dot{\bar{\varepsilon}}^{p})$ with plastic strain, Eq. (4), allows reducing the rate of the phase transformation by diminishing its intensity and delaying its starting point, Fig. 4a. Concerning the coefficient ξ, it controls the strain level where the phase transformation is observed on the macroscopic scale by σ–ε form. The phase transformation starts at determined initiation point of strain, Fig. 4b.

A parametric study is shown in the following curves to define how the shape of $h(\dot{\bar{\varepsilon}}^{p})$ changes with λ and the influence of ξ value on the kinetics of the phase transformation, Fig. 4a and b.

In order to define the influence of strain rate in the phase transformation process, the following relation in the form of Eq. (5) is proposed. It is observed that an increase of λ, Fig. 5, decreases the strain rate level where the phase transformation is annihilated. This coefficient can be identified using the experimental data in terms of macroscopic behaviour on the form of σ–ε curve

$$h(\dot{\bar{\varepsilon}}^{p}) = \lambda_0 \exp(-\lambda \dot{\bar{\varepsilon}}^{p}), \tag{5}$$

where λ_0 and λ are two shape fitting parameters which define the strain rate dependency on the phase transformation.

The effect of adiabatic temperature increase in dynamic conditions is taken into account in the model via the strain rate dependency of the flow stress.

In the following section the relation which defines the effect of initial temperature on the kinetics of phase transformation is discussed.

3.3. Definition of the effect of temperature in the phase transformation kinetics

Two formulations are proposed to define the influence of initial temperature on the phase transformation phenomena, Eqs. (6) and (7).

3.3.1. Temperature function based on M_S and M_D values

The first expression proposed $g_1(T)$, Eq. (6), is based on the relation proposed by Johnson and Cook [43] and similar to the formulation used to describe phase transformation process, for example, by Papatriantafillou et al. [1]

$$\begin{cases} g_1(T) = 1 - \Theta^{n} & \text{if } T \le M_S \rightarrow g_1(T) = 1, \\ \Theta = \left(\frac{T - M_S}{M_D - M_S}\right) & \text{if } T \le M_D \rightarrow g_1(T) = 0, \end{cases} \tag{6}$$

where $\Theta = (T - M_S)/(M_D - M_S)$ is the normalized temperature. The current temperature is T, M_S is the martensite-start temperature and M_D is the temperature at which the martensite cannot be induced, no matter how much the austenite is deformed [2]. The values of M_S and M_D must be obtained from experiments in quasi-static conditions. Moreover, η is the temperature sensitivity of the phase transformation.

A parametric study concerning η has been conducted in order to show the effect it has on the kinetics of phase transformation, Fig. 6a. As it is shown, Fig. 6a, it allows for description of the intensity and level of phase transformation depending on the initial temperature, T_0, in qualitative agreement with experimental observations, Fig. 6b, [11].

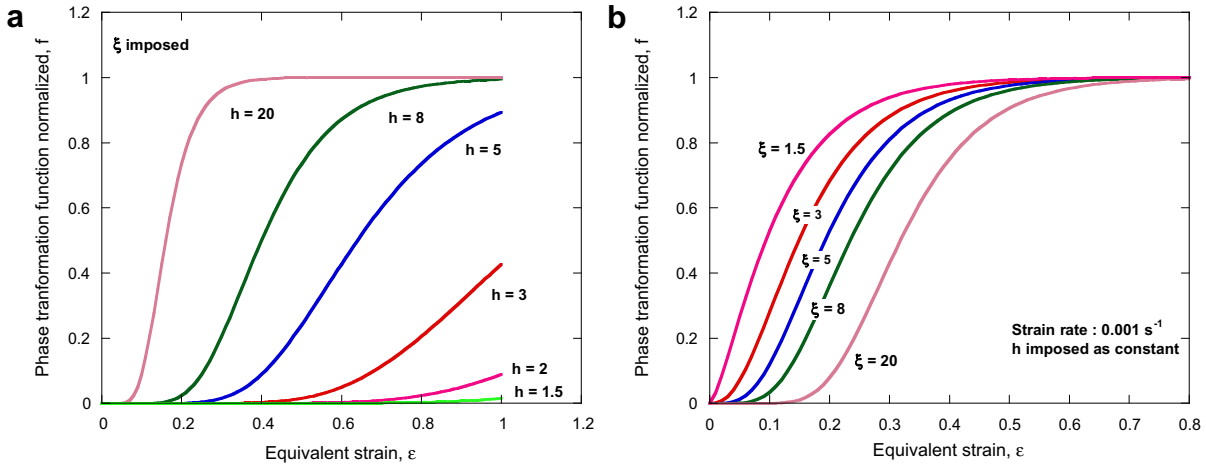

Fig. 4. Evolution of phase transformation function $f(\dot{\bar{\varepsilon}}^{p}, \bar{\varepsilon}^{p})$ with equivalent strain, (a) at fixed strain rate levels for different values of the function h, (b) for different values of ζ.

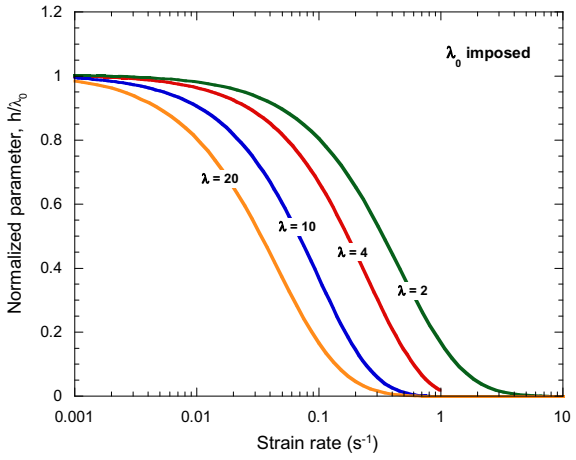

Fig. 5. Evolution of normalized parameter h/λ_0 with strain rate.

3.3.2. Temperature function based on exponential function

The second expression proposed $g_2(T)$, Eq. (7), is an exponential type equation similar to that reported by Mahnken et al. [25] and originally proposed in [44]

$$g_2(T) = \exp\left[-\left(\frac{T}{M_D - To}\right)^{\alpha}\right] \tag{7}$$

where T is the current temperature, To and α are material constants. The expression proposed is depending on M_D but not on M_S as previously. The M_D value must be obtained from experiments in quasi-static condition. For a given M_D there is just one possible combination of To and α values which fit the requirements of the phase transformation process, (if $T \geq M_D \rightarrow g_2(T) = 0$). For example in the case of $M_D = 300$ K, the parameters To and α take the values 80 K and 5, respectively, Fig. 7.

Thus, this type of function $g_2(T)$ is less flexible in comparison with $g_1(T)$ to define temperature effect. However, it allows defining temperature effect in the whole range of initial temperatures without imposing any restriction. It facilitates numerical computation.

4. Validation of the constitutive relation and comparison with experimental results

Analytical results of generalized model are compared with experiments for 301Ln2B steel [45]. This steel has been chosen since the process of phase transformation is well exposed by σ–ε curves at different initial strain rates, Fig. 8.

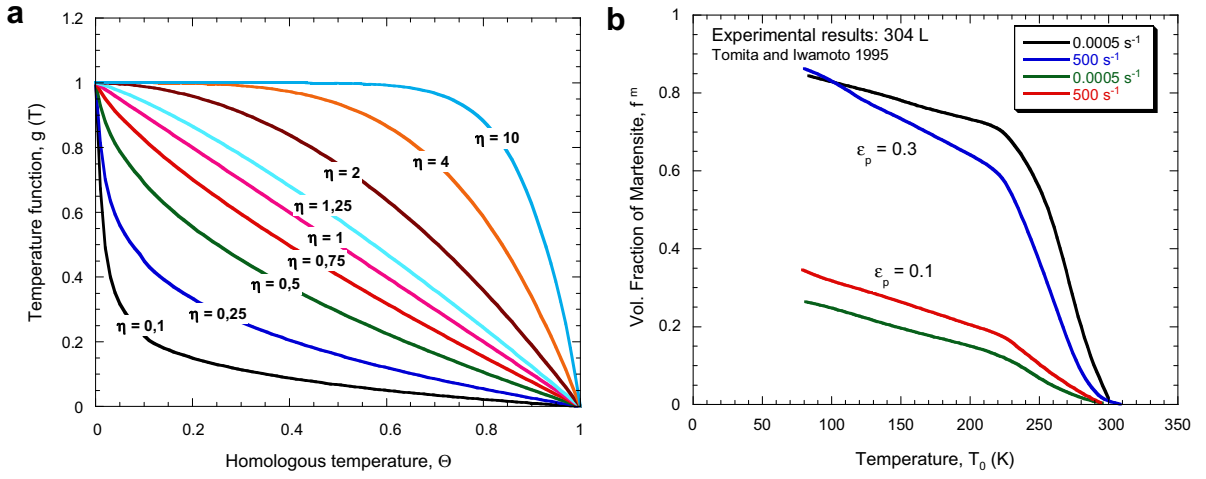

Fig. 6. (a) Evolution of temperature sensitivity with initial temperature for different values of η, (b) evolution of the volume fraction of martensite with temperature, experimental results [11].

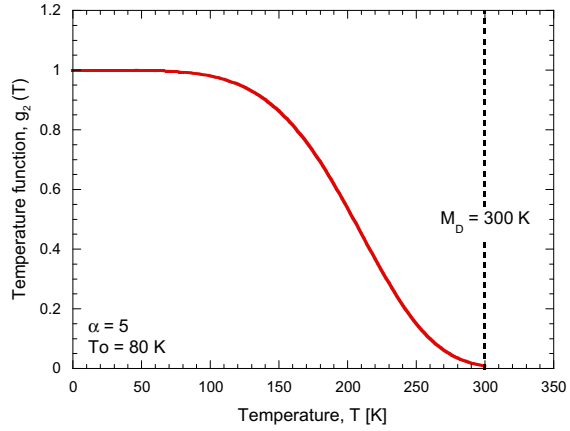

Fig. 7. Evolution of $g_2(T)$ function with temperature.

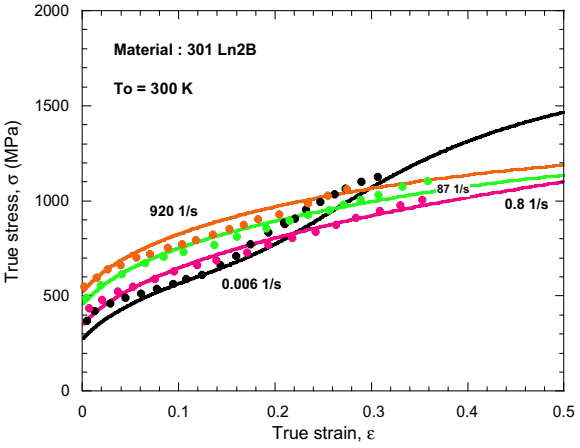

Fig. 8. Analytical predictions of the constitutive relation (solid lines) and comparison with experimental results [45].

Considering the results shown in Fig. 8, it is observed a satisfactory agreement between experimental results and analytical predictions for a wide range of strain rates within the range: $0.006 \leq \dot{\bar{\varepsilon}}^{p} \leq 920\ s^{-1}$. However, no comparison of the constitutive modeling with experimental results is conducted in terms of temperature sensitivity due to the lack of data for the material considered.

5. Analytical predictions of the modified RK constitutive relation

Using the phenomenological approach introduced in this paper, it is possible to approximate the influence of strain, strain rate and temperature on flow stress during plastic deformation together with phase transformation. Comparison between analytical predictions using original and generalized formulation of RK constitutive relation is shown in Fig. 9a and b. The results obtained using generalized formulation for different initial strain rate levels demonstrate the annihilation of phase transformation with strain rate increase, Fig. 9b.

In the following plot, Fig. 10a and b, is shown the response of the constitutive relation when a jump on strain rate is imposed at room temperature. In the case of a jump of strain rate from quasi-static to dynamic loading the model predicts correctly the annihilation of the phase transformation process when adiabatic conditions are reached.

In the opposite case, if the jump is conducted from dynamic to quasi-static strain rates, the model predicts the appearance of phase transformation process due to isothermal conditions.

The analytical predictions of the model in quasi-static conditions for several initial temperatures T_0, in the case of $g_1(T)$ using $\eta = 1$, and $g_2(T)$ using $To = 80$ K and $\alpha = 5$ are shown in Fig. 11a and b. A qualitative agreement was found with the experimental observations for several austenitic steels, Fig. 11c, [46]. When a certain value of initial temperature is high enough, the phase transformation is annihilated, Fig. 11a. The level of phase transformation increases when the temperature is close to M_S, Fig. 11a and b.

In the case $g_1(T)$ using $\eta = 1$, evolution of the rate of strain hardening $h(\bar{\varepsilon}_p) = \partial\bar{\sigma}/\partial\bar{\varepsilon}_p$ with plastic deformation for different normalized temperatures Θ is shown in Fig. 11d. An increase of strain hardening rate is observed during the phase transformation until a maximum is reached. This maximum is lower with an increase of the initial temperature. When the maximum is exceeded, the strain hardening rate starts to decrease continuously. Finally, it reaches a value close to the one which corresponds to strain hardening curves which previously have not shown the phase transformation.

6. Identification of material constants

It should be noticed that the functions $g_i(T)$ have not been calibrated for the material considered due to the absence of experimental data at different initial temperatures, $g_i(T) = 1$. In further analyses $g_i(T)$ should be taken into account in order to obtain a complete fitting of the material behaviour. The following values

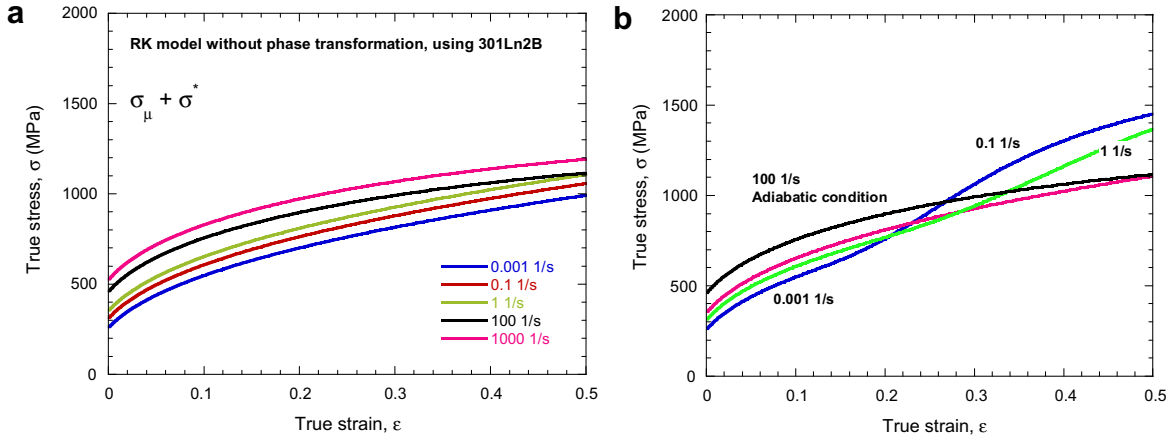

Fig. 9. Analytical predictions of the constitutive relation (a) original RK formulation without phase transformation. (b) Extended RK formulation, $g_i(T) = 1$.

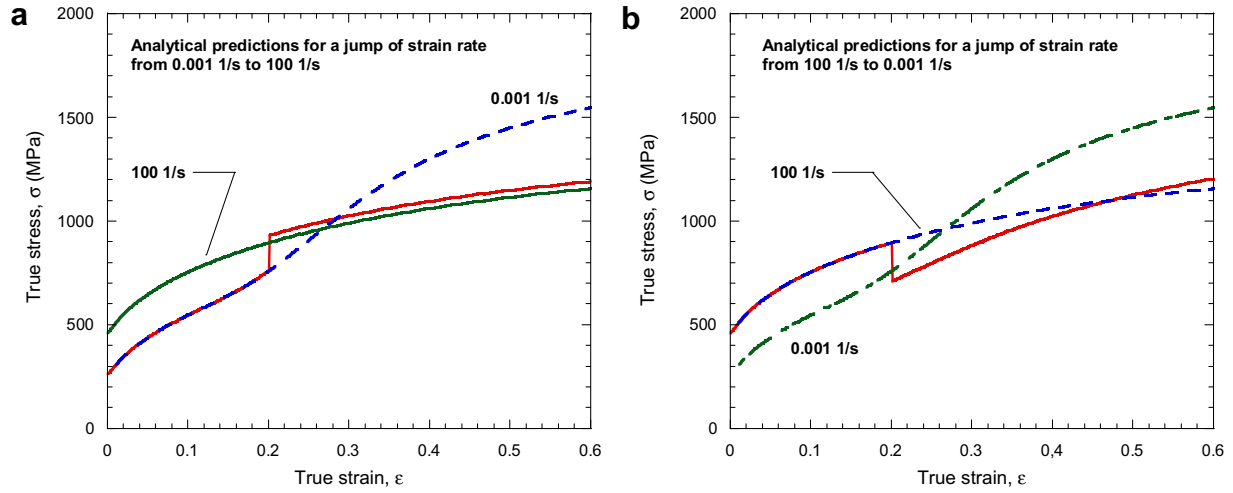

Fig. 10. Analytical predictions of the extended RK model in the case of (a) positive and (b) negative jump of strain rate for $g(T) = 1$.

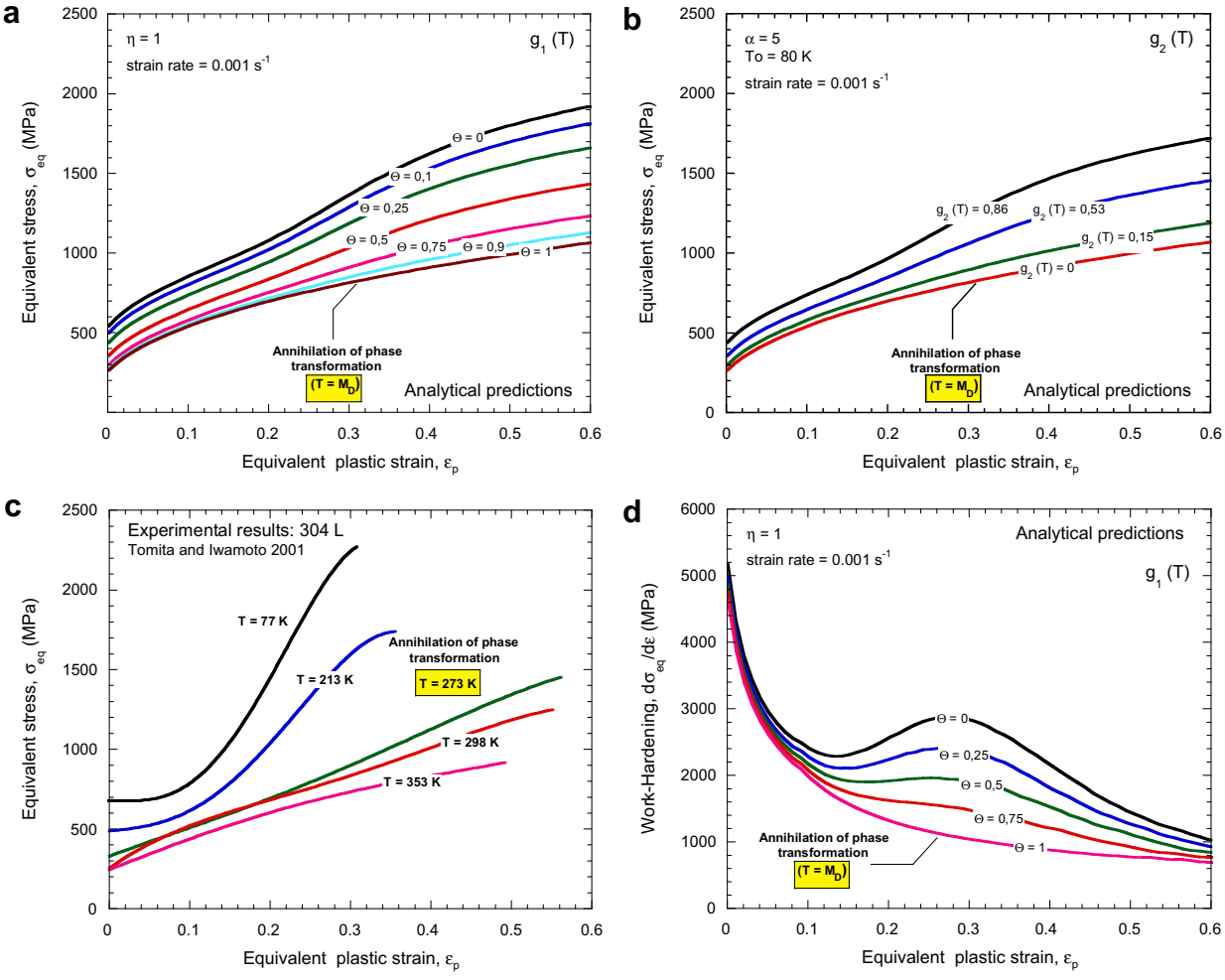

Fig. 11. Analytical predictions (a) in the case of $g_1(T)$ using $\eta = 1$ and (b) in the case of $g_2(T)$. (c) Experimental results [46] of stress vs. strain. (d) Analytical predictions of work-hardening vs. strain for different homologous temperatures, in the case of $g_1(T)$ $\eta = 1$.

of material constants, determined to account for the phase transformation in 301Ln2B at room temperature using experimental results [45], are given in Table 1. Those constants were implemented into the modified RK model. The constants used to define the original formulation of RK model are given in Table 2.

In order to determine the material constants cited in Table 1, the first stage is to suppose absence of phase transformation during plastic deformation. Next, the stress level is artificially increased with plastic deformation step by step after the point of initiation of the phase transformation, Fig. 12, by using a strain

Table 1
Additional material constants defining phase transformation for 301Ln2B steel.

σ_0 (MPa)	ξ	λ_0	λ
500	17	10	4

Table 2
Values of material constants in the original RK constitutive relation for 301Ln2B steel without phase transformation.

B_0 (MPa)	n_0 (–)	ν (–)	D_2 (–)	ε_0 (–)	σ_0^* (MPa)	m^* (–)	D_1 (–)
1380	0.41	0.1	0.05	0.018	488.33	1.66	0.52

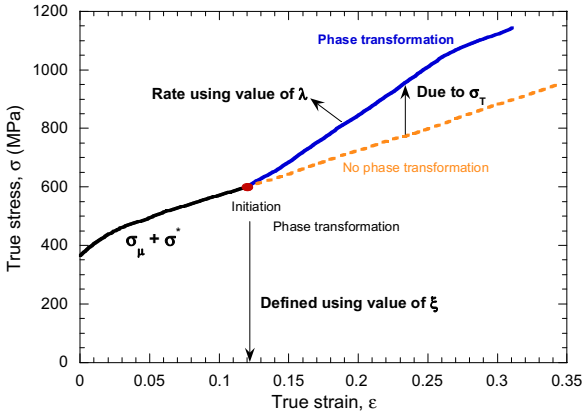

Fig. 12. Schematic representation of the method to determine the values of material constants in modified RK model using experimental results published in [45].

hardening initial curve obtained in quasi-static loading. This first step allows defining the hardening rate of material via the internal stress $\sigma_\mu(\bar{\varepsilon}_p, \dot{\bar{\varepsilon}}_p, T)$.

Subsequently, it is defined the dependency presented by yield stress $B(\dot{\bar{\varepsilon}}_p, T)$ and hardening coefficient $n(\dot{\bar{\varepsilon}}_p, T)$ on strain rate. This process is performed using stress–strain curves obtained for a strain level lower than phase transformation initiation point as shown in Fig. 12. Details concerning the process to obtain the values of material constants entering in the original formulation of the RK model can be found in [34]. Finally, the phase transformation effect is found by a quantitative analysis of the new stress component $\sigma_T(\bar{\varepsilon}_p, \dot{\bar{\varepsilon}}_p)$, Fig. 12. This is performed by subtracting the total stress $\bar{\sigma}_{eq}$ from the contribution of the internal stress $\sigma_\mu(\bar{\varepsilon}_p, \dot{\bar{\varepsilon}}_p, T)$ and the effective stress $\sigma^*(\dot{\bar{\varepsilon}}_p, T)$.

The number of material constants for the generalized model is not large. The total number is 12. It is also possible to determine explicitly the mathematical forms of the first derivatives of each stress components, Appendix B, which is useful for implementation of the constitutive relation into a FE code as reported in [30,31].

7. Conclusions

A phenomenological generalization of the RK model is reported in this paper. It includes behaviour of materials with phase transformation during plastic deformation as a function of strain, strain rate and temperature, $\sigma_T(\dot{\bar{\varepsilon}}^p, \bar{\varepsilon}^p, T)$. The key point of this generalized model is introduction of the shape function $f(\dot{\bar{\varepsilon}}^p, \bar{\varepsilon}^p)$ which approximates extra stress variations due to the phase transformation. The strain hardening and strain rate effects during phase transformation agree with experimental observations. To take into account the effect of initial temperature two different expressions have been defined, $g_i(T)$, based on expressions available in the open literature and in agreement with experimental observations.

An advantage in comparison with more sophisticated models for phase transformation process is the reduced number of constants. Another advantage is a simple way to determine all values of those material constants, the total number is twelve. In addition, the implementation into a FE code of this kind of phenomenological approach is relatively simple. It also allows for reduction of the computational time.

Appendix A. Complete formulation of the extended RK constitutive relation

$$\boxed{\bar{\sigma}(\bar{\varepsilon}_p, \dot{\bar{\varepsilon}}_p, T), = \tfrac{E(T)}{E_0}[\sigma_\mu(\bar{\varepsilon}_p, \dot{\bar{\varepsilon}}_p, T) + \sigma^*(\dot{\bar{\varepsilon}}_p, T)] + \sigma_T(\bar{\varepsilon}_p, \dot{\bar{\varepsilon}}_p, T)}, \tag{A.1}$$

- $$E(T) = E_0\left\{1 - \frac{T}{T_m}\exp\left[\theta^*\left(1 - \frac{T_m}{T}\right)\right]\right\}, \tag{A.2}$$
- $$\sigma_\mu(\bar{\varepsilon}_p, \dot{\bar{\varepsilon}}_p, T) = B(\dot{\bar{\varepsilon}}_p, T)(\varepsilon_0 + \bar{\varepsilon}_p)^{n(\dot{\bar{\varepsilon}}_p, T)}, \tag{A.3}$$
  - $$B(\dot{\bar{\varepsilon}}_p, T) = B_0\left(\left(\frac{T}{T_m}\right)\log\left(\frac{\dot{\varepsilon}_{max}}{\dot{\bar{\varepsilon}}_p}\right)\right)^{-\nu}, \tag{A.4}$$
  - $$n(\dot{\bar{\varepsilon}}_p, T) = n_0\left\langle 1 - D_2\left(\frac{T}{T_m}\right)\log\frac{\dot{\bar{\varepsilon}}_p}{\dot{\varepsilon}_{min}}\right\rangle, \tag{A.5}$$
- $$\sigma^*(\dot{\bar{\varepsilon}}_p, T) = \sigma_0^*\left\langle 1 - D_1\left(\frac{T}{T_m}\right)\log\left(\frac{\dot{\varepsilon}_{max}}{\dot{\bar{\varepsilon}}_p}\right)\right\rangle^{m^*}, \tag{A.6}$$
- $$\sigma_T(\dot{\bar{\varepsilon}}^p, \bar{\varepsilon}^p, T) = \sigma_0^\alpha \cdot f(\dot{\bar{\varepsilon}}^p, \bar{\varepsilon}^p) \cdot g(T), \tag{A.7}$$
  - $$f(\dot{\bar{\varepsilon}}^p, \bar{\varepsilon}^p) = [1 - \exp(-(\lambda_0 \exp(-\lambda\dot{\bar{\varepsilon}}^p)) \cdot \bar{\varepsilon}^p)]^\xi, \tag{A.8}$$
  - $$g_1(T) = 1 - \left(\frac{T - M_S}{M_D - M_S}\right)^\eta, \tag{A.9}$$
  - $$g_2(T) = \exp\left[-\left(\frac{T}{M_D - To}\right)^\alpha\right]. \tag{A.10}$$

Appendix B. Derivatives of the new stress component for implementation into FE code

$$\left.\frac{d\sigma_T\left(\dot{\bar{\varepsilon}}^p, \bar{\varepsilon}^p, T\right)}{d\bar{\varepsilon}^p}\right|_{\dot{\bar{\varepsilon}}^p, T} = \left\{\left[\xi \cdot \left[1 - \exp\cdot\left(\lambda_0 \cdot \exp\left(-\lambda\dot{\bar{\varepsilon}}^p\right) \cdot \bar{\varepsilon}^p\right)\right]^{\xi-1}\right] \cdot \left[-\exp\left(\left(-\lambda_0 \cdot \exp\left(-\lambda \cdot \dot{\bar{\varepsilon}}^p\right)\right) \cdot \bar{\varepsilon}^p\right)\right] \cdot \left[-\lambda_0 \cdot \exp\left(-\lambda \cdot \dot{\bar{\varepsilon}}^p\right)\right]\right\} \cdot g(T) \tag{B.1}$$

$$\left.\frac{d\sigma_T\left(\dot{\bar{\varepsilon}}^p, \bar{\varepsilon}^p, T\right)}{d\dot{\bar{\varepsilon}}^p}\right|_{\dot{\bar{\varepsilon}}^p, T} = \left\{\left[\xi \cdot \left[1 - \exp\left[-\lambda_0 \cdot \exp(-\lambda\dot{\bar{\varepsilon}}^p)\right] \cdot \bar{\varepsilon}^p\right]^{\xi-1}\right] \cdot \left[-\exp\left(-\lambda_0 \cdot \exp(-\lambda \cdot \dot{\bar{\varepsilon}}^p) \cdot \bar{\varepsilon}^p\right)\right] \cdot \left[-\lambda_0 \cdot \exp\left(-\lambda \cdot \dot{\bar{\varepsilon}}^p\right) \cdot \bar{\varepsilon}^p\right] \cdot [-\lambda]\right\} \cdot g(T) \tag{B.2}$$

$$g_1(T)\left\{\left.\frac{d\sigma_T\left(\dot{\bar{\varepsilon}}^p, \bar{\varepsilon}^p, T\right)}{dT}\right|_{\bar{\varepsilon}^p, \dot{\bar{\varepsilon}}^p} = \left\{\left[-\eta \cdot \left(\frac{T - M_s}{M_d - M_s}\right)^{\eta-1}\right] \cdot \left[\frac{1}{M_D - M_S}\right]\right\} \cdot f\left(\dot{\bar{\varepsilon}}^p, \bar{\varepsilon}^p\right) \tag{B.3}$$

$$g_2(T)\left\{\left.\frac{d\sigma_T\left(\dot{\bar{\varepsilon}}^p, \bar{\varepsilon}^p, T\right)}{dT}\right|_{\bar{\varepsilon}^p, \dot{\bar{\varepsilon}}^p} = \left\{\left[\exp\left[-\left(\frac{T}{M_D - To}\right)^\alpha\right]\right] \cdot \left[-\alpha \cdot \left(\frac{T}{M_D - To}\right)^{\alpha-1}\right] \cdot \left[\frac{1}{M_D - To}\right]\right\} \cdot f\left(\dot{\bar{\varepsilon}}^p, \bar{\varepsilon}^p\right) \tag{B.4}$$

References

[1] Papatriantafillou I, Agoras M, Aravas N, Haidemenopoulos G. Constitutive modeling and finite element methods for TRIP steels. Comput Methods Appl Mech Eng 2006;195:5094–114.
[2] Lebedev AA, Kosarchuk V. Influence of phase transformations on the mechanical properties of austenitic stainless steels. Int J Plasticity 2000;16:749–67.
[3] Bouaziz O, Guelton N. Modelling of TWIP effect on work-hardening. Mater Sci Eng A 2001;319–321:246–9.
[4] Nemat-Nasser S, Guo WG, Kihl DP. Thermo mechanical response of AL-6XN stainless steel over a wide range of strain rates and temperatures. J Mech Phys Solids 2001;49:1823–46.
[5] Abed FH, Voyiadjis GZ. Plastic deformation modelling of AL-6XN stainless steel at low and high strain rates and temperatures using a combination of bcc and fcc mechanisms of metals. Int J Plasticity 2005;21:1618–39.
[6] Guo WG, Nemat-Nasser S. Flow stress of Nitronic-50 stainless steel over a wide range of strain rates and temperatures. Mech Mater 2006;38:1090–103.
[7] Bouaziz O, Allain S, Scott C. Effect of grain and twin boundaries on the hardening mechanisms of twinning induced plasticity steels. Scripta Mater 2008;58:484–7.
[8] Larour P, Rusinek A, Klepaczko JR, Beck W. Effects of strain rate and identification of material constants for three automotive steels. Steel Res Int 2007;78:348–58.
[9] Olson GB, Cohen M. Kinematics of strain-induced martensitic nucleation. Metall Trans A 1975;6:791–5.
[10] Stringfellow RG, Parks DM, Olson GB. A constitutive model for transformation plasticity accompanying strain-induced martensitic transformation in meta-stable austenitic steels. Acta Metall 1992;40:1703–16.
[11] Tomita Y, Iwamoto T. Constitutive modelling of TRIP steel and its application to the improvement of mechanical properties. Int J Mech Sci 1995;37:1295–305.
[12] Iwamoto T, Tsuta T, Tomita Y. Investigation on deformation mode dependence of strain-induced martensitic transformation in TRIP steels and modelling of transformation kinetics. Int J Mech Sci 1998;40:173–82.
[13] Iwamoto T, Tsuta T. Computational simulation of the dependence of the austenitic grain size on the deformation behavior of TRIP steels. Int J Plasticity 2000;16:791–804.
[14] Taleb L, Petit S. New investigations on transformation induced plasticity and its interaction with classical plasticity. Int J Plasticity 2006;22:110–30.
[15] Meftah S, Barbe F, Taleb L, Sidoroff F. Parametric numerical simulations of TRIP and its interaction with classical plasticity in martensitic transformation. Eur J Mech A Solids 2007;26:688–700.
[16] Huha H, Seok-Bong Kima SB, Songa JH, Lim JH. Dynamic tensile characteristics of TRIP-type and DP-type steel sheets for an auto-body. Int J Mech Sci. doi:10.1016/j.ijmecsci.2007.09.004.
[17] Leblond JB, Mottet G, Devaux JC. A theoretical and numerical approach to the plastic behaviour of steels during phase transformations—I. Derivation of general relations. J Mech Phys Solids 1986;34:395–409.
[18] Leblond JB, Mottet G, Devaux JC. A theoretical and numerical approach to the plastic behaviour of steels during phase transformations—II. Study of classical plasticity for ideal-plastic phases. J Mech Phys Solids 1986;34:410–32.
[19] Fischer FD. A micromechanical model for transformation plasticity in steels. Acta Metall Mater 1990;38:1535–46.
[20] Fischer FD. Transformation induced plasticity in triaxiality loaded steel specimens subjected to a martensitic transformation. Eur J Mech A/Solids 1992;11:233–44.
[21] Fischer FD, Sun QP, Tanaka K. Transformation-induced plasticity (TRIP). Appl Mech Rev 1996;49:317–64.
[22] Cherkaoui M, Berveiller M, Sabar H. Micromechanical modelling of martensitic transformation induced plasticity (TRIP) in austenitic single crystals. Int J Plasticity 1998;14:597–626.
[23] Cherkaoui M, Berveiller M, Lemoine X. Coupling between plasticity and martensitic phase transformation: overall behavior of polycrystalline TRIP steels. Int J Plasticity 2000;16:1215–41.
[24] Delannay L, Jacques P, Pardoen T. Modelling of the plastic flow of trip-aided multiphase steel based on an incremental mean-field approach. Int J Solids Struct 2008;45:1825–43.
[25] Mahnken R, Schneidt A, Antretter T. Macro modelling and homogenization for transformation induced plasticity of a low-alloy steel. Int J Plasticity, in press. doi:10.1016/j.ijplas.2008.03.005.
[26] Aravas N. On the numerical integration of a class of pressure-dependent plasticity models. Int J Numer Methods Eng 1987;24:1395–416.
[27] Rusinek A, Klepaczko JR. Shear testing of sheet steel at wide range of strain rates and a constitutive relation with strain-rate and temperature dependence of the flow stress. Int J Plasticity 2001;17:87–115.
[28] Zaera R, Fernández-Sáez J. An implicit consistent algorithm for the integration of thermoviscoplastic constitutive equations in adiabatic conditions and finite deformations. Int J Solids Struct 2006;43:1594–612.
[29] Rusinek A, Zaera R, Klepaczko JR, Cheriguene R. Analysis of inertia and scale effects on dynamic neck formation during tension of sheet steel. Acta Mater 2005;53:5387–400.
[30] Rusinek A, Zaera R. Finite element simulation of steel ring fragmentation under radial expansion. Int J Impact Eng 2007;34:799–822.
[31] Rusinek A, Zaera R, Klepaczko JR. Constitutive relations in 3-D for a wide range of strain rates and temperatures – application to mild steels. Int J Solids Struct 2007;44:5611–34.
[32] Rusinek A, Zaera R, Forquin P, Klepaczko JR. Effect of plastic deformation and boundary conditions combined with elastic wave propagation on the collapse site of a crash box. Thin-Walled Struct 2008;46:1143–63.
[33] Rusinek A, Rodríguez-Martínez JA, Zaera R, Klepaczko JR, Arias A, Sauvelet C. Experimental and numerical study on the perforation process of mild steel sheets subjected to perpendicular impact by hemispherical projectiles. Int J Impact Eng 2008. doi:10.1016/j.ijimpeng.2008.09.00.
[34] Klepaczko JR, Rusinek A, Rodríguez-Martínez JA, Pęcherski RB, Arias A. Modelling of thermo-viscoplastic behaviour of DH-36 and Weldox 460-E structural steels at wide ranges of strain rates and temperatures, comparison of constitutive relations for impact problems. Mech Mater, submitted for publication.
[35] Zaera R. Internal Report. Implementación numérica de modelos de comportamiento de materiales metálicos avanzados para diseño de sistemas de absorción de energía en choques. Department of Continuum Mechanics and Structural Analysis. University Carlos III of Madrid. Spanish Ministry of Education (Project DPI2005-06769), 2008.
[36] Durrenberger L, Even D, Molinari A, Rusinek A. Influence of the strain path on crash properties of a crash-box structure by experimental and numerical approaches. J Phys IV 2006;134:1287–93.
[37] Rusinek A, Klepaczko JR. Experiments on heat generated during plastic deformation and stored energy for TRIP steels. Mater Design 2009;30:35–48.
[38] Klepaczko JR. A general approach to rate sensitivity and constitutive modeling of FCC and BCC metals. In: Impact: effects of fast transient loadings. Rotterdam: A.A. Balkema; 1998. p. 3–35.
[39] Rusinek A, Rodriguez-Martinez JA, Klepaczko JR, Pęcherski RB. Analysis of thermo-visco-plastic behaviour of six high strength steels. J Mater Design 2009;30:1748–61.
[40] Berbenni S, Favier V, Lemoine X, Berveiller N. Micromechanical modelling of the elastic-viscoplastic behaviour of polycrystalline steels having different microstructures. Mater Sci Eng 2004;372:128–36.
[41] Pęcherski RB. Macroscopic effect of micro-shear banding in plasticity of metals. Acta Mech 1998;131:203–24.
[42] Pęcherski RB. Continuum mechanics description of plastic flow produced by micro-shear bands. Tech Mech 1998;18:107–15.
[43] Johnson GR, Cook WH. A constitutive model and data for metals subjected to large strains, high strain rates and high temperatures. In: Proceedings of 7th international symposium on ballistics, 1983. p. 541–7.
[44] Koistinen DP, Marburger RE. A general equation prescribing the extent of the austenite–martensite transformation in pure iron–carbon alloys and plain carbon steels. Acta Mater 1959;7:59–60.
[45] Larour P, Verleysen P, Bleck W. Influence of uniaxial, biaxial and plane strain pre-straining on the dynamic tensile properties of high strength sheet steels. J Phys IV 2006;134:1085–90.
[46] Tomita Y, Iwamoto T. Computational prediction of deformation behaviour of TRIP steels under cyclic loading. Int J Mech Sci 2001;43:2017–34.